

may as well isomerize into 4 (a lower critical energy process) and further into 2. These successive isomerizations bring about the mixing of the original proton (labeled with a star in Scheme IV) with four of the five H atoms of the ethyl chain. The results above indicate that only roughly half of the ions 1 react by specific  $\beta$ -elimination.

Moreover, the H-randomization also seems to involve, to some extent, the first H transferred during step 1  $\rightarrow$  3. This observation may be accounted for by a partial reversibility of reaction 1  $\rightarrow$  3 for metastable ions 1. Another possibility is the isomerization of 3 or 4 into the cyclic structure  $[\text{HC}=\text{NH}-\text{CH}_2-\text{CH}_2]^+$  (10) followed by C-C ring opening and 1,2 H migration leading to  $[\text{CH}_2\text{C}=\text{NCH}_3]^+$ . It is difficult to evaluate the role of this reversibility as it is only evidenced by low intensity signals ( $m/z$  30 for 1b, 1c, and  $m/z$  28 for 1d and 1e) and a fortiori to answer with certainty the latter question.

Ions 1 of higher internal energy dissociate into  $\text{C}_2\text{H}_5^+$  ions. It is proposed that, in view of the energy gap between 6 and 7, only the products 6 can be obtained after the sequence 1  $\rightarrow$  3  $\rightarrow$  4  $\rightarrow$  2  $\rightarrow$  6 (Scheme IV). This may explain the similar abundance ratios ( $m/z$  28)/( $m/z$  29) observed in both MIKE spectra of 1 and 2. Note that the internal energy content of the metastable ions 1 leading to 6 is sufficient to allow the reversibility of the first step 3  $\rightarrow$  1. Thus the C-bonded H atom in  $\text{HCNH}^+$  is also mixed to some extent with the other five H atoms, and consequently signals corresponding to  $\text{C}_2\text{H}_5^+$  must involve statistically all H of the precursor ion 1 as corroborated by experiment (see, for example,  $m/z$  32 and 31 in 1c).

### Conclusion

The reactivity of low energy both protonated ethyl cyanide (1) and ethyl isocyanide (2) may be conveniently described by the

energy profile in Figure 2; both species interconvert through  $\pi$ -bonded complexes 3 and 4 differing in the mutual orientation of the partners by 180° before their decomposition either into  $\text{NCNH}^+$  and ethene, or into  $\text{C}_2\text{H}_5^+$  and HCN. The interconversion 3  $\rightleftharpoons$  4 requires either the intermediacy of more energetized ion neutral complex structures (less than 224 kJ mol<sup>-1</sup> though), satisfying the so-called "reorientation criterion",<sup>31</sup> or the addition of the partners into a more stable transient cyclic immonium ion.

The present data also provide new insight into the chemistry of  $\text{C}_3\text{H}_6\text{N}^+$  ions from which  $\text{C}_2\text{H}_5\text{CN}$  (or  $\text{C}_2\text{H}_5\text{NC}$ ) may originate via dissociative recombination in interstellar media. It has been shown that isomerization 1  $\rightleftharpoons$  2 requires ca. 250 kJ mol<sup>-1</sup> (Figure 2). Consequently, ion 1 whose internal energy is lower than 250 kJ mol<sup>-1</sup> will produce only  $\text{C}_2\text{H}_5\text{CN}$  molecules by the reaction 1 + e  $\rightarrow$   $\text{C}_2\text{H}_5\text{CN}$  + H<sup>\*</sup>, while the more energetic ions 1 are likely to produce a mixture of  $\text{C}_2\text{H}_5\text{CN}$  and  $\text{C}_2\text{H}_5\text{NC}$ . Hence, whether  $\text{C}_2\text{H}_5\text{NC}$  exists in interstellar clouds along with  $\text{C}_2\text{H}_5\text{CN}$  strongly depends on the internal energy content of 1 and thereby on its origin whose knowledge is crucial.

Further work is in progress on other  $\text{C}_3\text{H}_6\text{N}^+$  isomers such as  $[\text{CH}_2=\text{CH}-\text{CH}=\text{NH}_2]^+$  and higher homologues in order to get a deeper understanding of the complex chemistry of these ionic species.

**Acknowledgment.** M.T.N. is a Research Associate of the National Fond for Scientific Research (NFWO, Belgium). We thank the Ecole Polytechnique for financial support and KU Leuven for a grant of computer time.

(31) (a) Bowen, R. D. *Acc. Chem. Res.* 1991, 24, 364. (b) Morton, T. H. *Org. Mass Spectrom.* 1992, 27, 353. (c) Longevialle, P. *Mass Spectrom. Rev.* 1992, 11, 157.

## Cation-Framework Interaction in Alkali-Cation-Exchanged Zeolites: An XPS Study

M. Huang, A. Adnot, and S. Kaliaguine\*

Contribution from the Département de Génie Chimique et CERPIC, Université Laval, Québec, Canada. Received May 18, 1992

**Abstract:** A series of alkali-cation-exchanged and also some proton-exchanged zeolites have been investigated using XPS. The larger the electropositivity of the counterion is, the lower the framework element ( $\text{Si}_{2p}$ ,  $\text{Al}_{2p}$ , and  $\text{O}_{1s}$ ) binding energies are. However, the extent of these changes depends strongly on the Si/Al ratio of zeolites. On the basis of the changes in  $\text{N}_{1s}$  binding energy and previous infrared results for the chemisorbed pyrrole probe molecule, evidence is offered to support the hypothesis that the cation-framework interaction in zeolites is limited to a short-range scope. On the basis of this kind of short-range interaction, a model for pyrrole chemisorption is suggested and the charges on N, Si, and Al are then calculated using the Sanderson electronegativity equalization method. The calculated charges correlate well with the observed binding energies of the corresponding elements. The results further suggest that the probe molecules containing N atoms are sensitive indicators of charge transfer in XPS experiments. The  $\text{Si}_{2p}$  binding energy level is not a good internal reference binding energy in XPS spectra for zeolites possessing a low Si/Al ratio.

### Introduction

The bonding chemistry in zeolites has been discussed by Mortier and Schoonheydt.<sup>1</sup> Using Gutmann's interatomic interaction rules and the Sanderson electronegativity equalization principle, they proposed an electron donor-acceptor interaction between the extraframework cations and the framework atoms. The same topic was also investigated by Barr,<sup>2</sup> on the basis of a series of XPS studies.<sup>2-4</sup> A group shift concept is suggested to explain why the binding energies of all zeolite elements shift in the same direction

with a change in the Si/Al ratio. According to this concept, the two groups involved in zeolites are silica ( $\text{SiO}_2$ ) and metal aluminate. The formation of zeolites from these two groups will result in an increase in binding energies of all zeolite elements with an

- (1) Mortier, W. J.; Schoonheydt, R. A. *Prog. Solid State Chem.* 1985, 16, 1.  
 (2) Barr, T. L. *Zeolites* 1990, 10, 760.  
 (3) Barr, T. L. In *Practical Surface Analysis*; Briggs, D., Seah, M. P., Eds.; John Wiley: Chichester, U.K., 1983; Chapter 8.  
 (4) Barr, T. L.; Lishka, M. A. *J. Am. Chem. Soc.* 1986, 108, 3178.

\* To whom correspondence should be addressed.

increase in Si/Al ratio. The change in binding energy of zeolite elements with the change in Si/Al ratio was also observed by Okamoto<sup>5</sup> and Stoch<sup>6</sup> et al. Stoch et al. however found that the Al<sub>2p</sub> binding energy did not depend on or slightly increased with Al content, which is the opposite of most literature results. Moreover, electron polarization and the charge transfer between Al<sub>2</sub>O<sub>3</sub> and SiO<sub>2</sub> cannot explain the lower Al<sub>2p</sub> binding energy in some zeolites compared to that in Al<sub>2</sub>O<sub>3</sub> (74.3–74.7 eV<sup>7</sup>). Apparently, the group shift concept is a better explanation, consistent with the Sanderson electronegativity equalization principle. We want to point out that the group shift concept can be suitable whether the short-range or the long-range aspect of bonding chemistry is emphasized. According to our understanding, however, the bonding between framework elements should be different from that between extraframework cations and the framework. In fact, the long-range symmetry of zeolite crystallinity indicates the importance of the long-range aspect of chemical bonding between framework elements, which results in the additional long-range stability of the zeolite structure.<sup>1,8</sup> On the other hand, as the interaction between extraframework cations and the framework varies from site to site,<sup>9</sup> the local environment, or the short-range aspect, in this kind of interaction should become important. In this work, a series of alkali-cation-exchanged and also some proton-exchanged zeolites were investigated using XPS, the results of which were combined with previous infrared results.<sup>10</sup> Evidence is offered to support the hypothesis that the cation-framework interaction in zeolites is limited to a short-range scope.

### Experimental Section

Various alkali-cation-exchanged faujasite, mordenite, and ZSM-5 zeolites were prepared from the sodium forms contacted with the corresponding chloride solution, while the alkali-cation-exchanged L zeolites were prepared from the potassium forms. The exchange temperature was maintained at 70–80 °C, and the time for a single exchange was around 24 h. In most cases, up to three successive exchanges were performed in order to obtain high exchange levels. HX zeolites were obtained by calcination of NH<sub>4</sub><sup>+</sup>-exchanged X zeolites at 300 °C. Details of the preparation of HZSM-5 have been previously described.<sup>11</sup> The bulk chemical composition of zeolites was established by atomic absorption spectroscopy using a Perkin-Elmer (Model 1100B) spectrometer. The results revealed that the exchange level of alkali cations is 100% for ZSM-5 samples but less than 100% for other zeolites.<sup>10</sup>

Gold deposited onto fresh zeolite samples was used as a calibrant for determining the absolute binding energies in the XPS experiments (Au<sub>4f<sub>7/2</sub></sub> = 84.0 eV). The deposition was performed under vacuum (10<sup>-3</sup> Torr), and the thickness of gold layers was around 20 Å. The XPS spectra of pyrrole chemisorbed samples were also recorded for alkali-cation-exchanged X and Y zeolites. In this experiment, the zeolite samples were pressed into self-supported wafers of roughly 10 mg. The samples were degassed at 400 °C overnight and then cooled in vacuum (10<sup>-5</sup> Torr) to 65 °C. The pyrrole vapor was introduced at this temperature for 2 h. The XPS spectra for pyrrole chemisorbed samples were recorded at liquid nitrogen temperature (–196 °C) in order to avoid the easy desorption of chemisorbed pyrrole under the high vacuum of the spectrometer chamber (less than 10<sup>-8</sup> Torr). For these samples, the C<sub>1s</sub> level (284.4 eV) was taken as the reference binding energy. A VG Scientific Escalab Mark II system with a hemispherical analyzer operating in the constant-pass energy mode (20 eV) was employed. A Mg Kα X-ray source (hν = 1253.6 eV) was operated at 20 mA and 15 kV. N<sub>1s</sub> peaks were deconvoluted into two or three components by keeping the same value for the full width at half-maximum (fwhm) of all component peaks in a particular spectrum and assuming that the component peaks had Gaussian–Lorentzian shape. In this deconvolution operation, the fwhm value

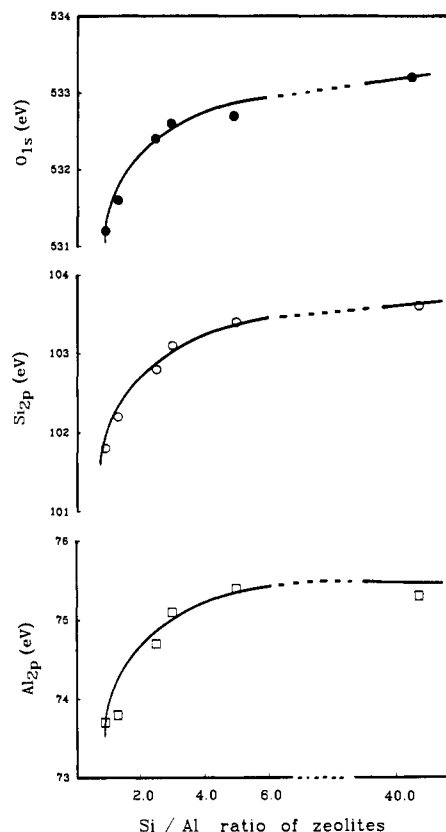


Figure 1. Chemical change in binding energies of Na zeolites with the Si/Al ratio of the zeolite framework.

adopted for all the component peaks of the N<sub>1s</sub> lines was 2.4 eV.

### Results and Discussion

Table I summarizes the binding energies of zeolite samples observed in this work. For comparison, the data found in refs 4 and 5 are also listed in the table. The present results of fresh samples are consistent with most literature data and extend to zeolite L and three complete series of alkali-cation-exchanged zeolites (X, Y, and ZSM-5). When zeolites containing the same alkali cation, such as the sodium form of zeolites (Figure 1), are compared, all the binding energies of framework elements increase with the Si/Al ratio. Okamoto<sup>5</sup> reported that the chemical shift between Al/Si = 0 and 1 depends strongly on the constituting elements and decreases in the order O<sub>1s</sub> > Si<sub>2s</sub> > Na<sub>1s</sub> > Al<sub>2p</sub>. In our case, this order is O<sub>1s</sub> > Si<sub>2p</sub> > Al<sub>2p</sub>. The same order was also observed by Barr and Lishka.<sup>4</sup> The more significant change observed in Si<sub>2p</sub> binding energy compared to Al<sub>2p</sub> binding energy was explained by the fact that the oxygen in an oxide prefers the ionic status to the covalent one. Therefore, in the –Si–O–Al– structure, the more ionic Al will induce a larger shift of Si<sub>2p</sub> binding energy. It is further noted that the fwhm of XPS lines are also reduced in the same order, O<sub>1s</sub> (around 2.7 eV) > Si<sub>2p</sub> (around 2.4 eV) > Al<sub>2p</sub> (around 2.2 eV).

The most interesting feature is the chemical shift in Si<sub>2p</sub>, Al<sub>2p</sub>, and O<sub>1s</sub> binding energies with different alkali cations. Figure 2 shows that the larger the electropositivity of the counterion, the lower the framework element (Si<sub>2p</sub>, Al<sub>2p</sub>, and O<sub>1s</sub>) binding energies. However, these changes are also strongly correlated with the Si/Al ratio of zeolites. The most significant shift was found in X and A zeolites, which possess a lower Si/Al ratio (1.25 and 0.88, respectively). This shift is smaller for Y zeolites. Finally, the change in binding energy with the alkali cations becomes negligible in ZSM-5 zeolites, which possess a high Si/Al ratio (40.7). At least one conclusion can be drawn here before further discussion. The Si<sub>2p</sub> binding energy level is not a good internal reference binding energy in XPS spectra for zeolites possessing low Si/Al ratios; however, it can be used as an internal reference binding energy for the high-silica-content zeolites.

(5) Okamoto, Y.; Ogawa, M.; Maezawa, A.; Imanaka, T. *J. Catal.* **1988**, *112*, 427.

(6) Stoch, J.; Lercher, J.; Ceckiewicz, S. *Zeolites* **1992**, *12*, 81.

(7) Wagner, C. D.; Riggs, W. M.; Davis, L. E.; Moulder, J. F. *Handbook of X-ray Photoelectron Spectroscopy*; Perkin-Elmer Corp.: Eden Prairie, MN, 1979.

(8) Rabo, J. A.; Gajda, G. J. *Catal. Rev.—Sci. Eng.* **1990**, *31*, 385.

(9) Mortier, W. J. *Compilation of Extra Framework Sites in Zeolites*; Butterworths: Guildford, U.K., 1982.

(10) Huang, M.; Kaliaguine, S. *J. Chem. Soc., Faraday Trans.* **1992**, *88*, 751.

(11) Borade, R.; Sayari, A.; Adnot, A.; Kaliaguine, S. *J. Phys. Chem.* **1990**, *94*, 5989.

Table I. XPS Results

sample <sup>a</sup>	unit cell cation compn	binding energy (fwhm), eV			
		Si <sub>2p</sub>	Al <sub>2p</sub>	O <sub>1s</sub>	N <sub>1s</sub>
NaA	Na <sub>12,8</sub>	101.8 (2.3)	73.7 (2.4)	531.2 (2.6)	
		100.9 <sup>d</sup>	73.2 <sup>d</sup>	530.2 <sup>d</sup>	
		101.7 <sup>e</sup>	73.7 <sup>e</sup>	531.0 <sup>e</sup>	
CsX-2 (p)	Cs <sub>28,8</sub> Na <sub>56,6</sub>	101.6 (2.4)	73.9 <sup>b</sup>	531.3 (2.6)	
		101.6 (2.4)	73.7 <sup>b</sup>	530.9 (2.5)	398.9 (3.3)
RbX (p)	Rb <sub>37,7</sub> Na <sub>47,7</sub>	101.8 (2.5)	73.9 (2.2)	531.3 (2.6)	
		101.7 (2.4)	73.6 (2.1)	530.9 (2.5)	399.3 (3.3)
KX (p)	K <sub>48,3</sub> Na <sub>37,1</sub>	101.8 (2.1)	74.0 (2.0)	531.2 (2.5)	
		101.8 (2.2)	73.7 (2.1)	530.9 (2.3)	399.5 (3.2)
		102.0 <sup>e</sup>	74.0 <sup>e</sup>	531.3 <sup>e</sup>	
NaX (p)	Na <sub>85,4</sub>	102.2 (2.2)	73.8 (2.1)	531.6 (2.3)	
		102.2 (2.3)	74.0 (2.1)	531.2 (2.3)	399.9 (2.7)
		101.8 <sup>d</sup>	73.7 <sup>d</sup>	530.9 <sup>d</sup>	
		101.9 <sup>e</sup>	74.1 <sup>e</sup>	531.1 <sup>e</sup>	
LiX (p)	Li <sub>54,3</sub> Na <sub>31,1</sub>	102.6 (2.2)	74.7 (2.2)	532.0 (2.5)	
		102.5 (2.2)	74.5 (2.1)	531.6 (2.3)	400.0 (3.0)
		102.4 <sup>e</sup>	74.1 <sup>e</sup>	531.6 <sup>e</sup>	
HX	H <sub>49,7</sub> Na <sub>35,7</sub>	102.7 (2.3)	74.9 (2.3)	532.0 (2.5)	
		102.7 <sup>e</sup>	74.9 <sup>e</sup>	532.2 <sup>e</sup>	
CsY (p)	Cs <sub>37,0</sub> Na <sub>17,5</sub>	102.2 (2.3)	73.7 <sup>b</sup>	531.4 (2.6)	
		102.3 (2.3)	73.9 <sup>b</sup>	531.4 (2.7)	399.6 (3.7)
		102.3 <sup>e</sup>	74.0 <sup>e</sup>	531.5 <sup>e</sup>	
RbY (p)	Rb <sub>34,3</sub> Na <sub>20,2</sub>	102.5 (2.4)	74.4 (2.2)	531.9 (2.7)	
		102.5 (2.3)	74.3 (2.1)	531.7 (2.6)	400.0 (3.0)
KY (p)	K <sub>40,0</sub> Na <sub>14,5</sub>	102.8 (2.2)	74.3 (2.2)	532.2 (2.7)	
		102.6 (2.3)	74.3 (2.1)	531.9 (2.6)	400.2 (3.9)
		102.5 <sup>e</sup>	74.0 <sup>e</sup>	531.9 <sup>e</sup>	
NaY (p)	Na <sub>54,5</sub>	102.8 (2.5)	74.7 (2.1)	532.4 (2.6)	
		102.7 (2.3)	74.4 (2.1)	532.1 (2.5)	400.2 (3.1)
		102.4 <sup>d</sup>	74.0 <sup>d</sup>	531.6 <sup>d</sup>	
		102.5 <sup>e</sup>	74.2 <sup>e</sup>	531.8 <sup>e</sup>	
LiY (p)	Li <sub>27,8</sub> Na <sub>26,7</sub>	102.8 (2.5)	c	532.3 (2.8)	
		102.8 (2.3)	75.0 (2.1)	532.3 (2.5)	400.1 (2.9)
		102.7 <sup>e</sup>	74.5 <sup>e</sup>	532.2 <sup>e</sup>	
NaL	Na <sub>8,0</sub> K <sub>0,9</sub>	103.1 (2.5)	75.1 <sup>b</sup>	532.6 (2.7)	
NaM	Na <sub>7,9</sub>	103.4 (2.5)	75.4 <sup>b</sup>	532.7 (2.7)	
CsZ	Cs <sub>2,3</sub>	103.5 (2.5)	75.4 <sup>b</sup>	533.1 (2.5)	
RbZ	Rb <sub>2,3</sub>	103.7 (2.4)	c	533.2 (2.4)	
KZ	K <sub>2,3</sub>	103.7 (2.4)	75.4	533.2 (2.6)	
NaZ	Na <sub>2,3</sub>	103.6 (2.3)	75.3 <sup>b</sup>	533.2 (2.5)	
LiZ	Li <sub>2,3</sub>	103.7 (2.4)	75.2 <sup>b</sup>	533.3 (2.4)	
HZ	H <sub>2,3</sub>	103.7 (2.6)	75.6 <sup>b</sup>	533.1 (2.5)	

<sup>a</sup>(p) = samples after pyrrole chemisorption. <sup>b</sup>The Al<sub>2p</sub> binding energy was estimated from the Al<sub>2s</sub> level, because of an overlapping of Al<sub>2p</sub> and Cs<sub>4d</sub> lines for the Cs zeolites and the overlapping of weak Al<sub>2p</sub> lines and the satellite line of Au<sub>4f</sub> for the fresh high-silica zeolites. (BE(Al<sub>2s</sub>) - BE(Al<sub>2p</sub>) = 44.9 eV.) <sup>c</sup>Not measured.

At first glance, the alkali-cation-dependent chemical shift in different zeolites can be explained by the Sanderson electronegativity equalization principle.<sup>12</sup> According to this principle, the intermediate electronegativity of zeolites is

$$S_{\text{int}} = (S_{\text{Si}}^p S_{\text{Al}}^q S_{\text{O}}^r S_{\text{M1}}^{n1} S_{\text{M2}}^{n2})^{1/(p+q+r+n1+n2)} \quad (1)$$

Hence the charge on Si(Al,O) can be calculated as

$$\delta_{\text{Si(Al,O)}} = (S_{\text{int}} - S_{\text{Si(Al,O)}}) / 2.08 S_{\text{Si(Al,O)}}^{1/2} \quad (2)$$

where M1 and M2 represent the two monovalent extraframework cations present in the zeolites, and *p*, *q*, *r*, *n1*, and *n2* are the chemical composition indexes of corresponding elements in zeolites. Assuming there is no extraframework Al, *q* is equal to *n1*+*n2*. Apparently, when the Si/Al ratio becomes high, the change in *S*<sub>M1</sub><sup>*n1*</sup> or *S*<sub>M2</sub><sup>*n2*</sup> will just result in a slight change in *S*<sub>int</sub>, and then a slight change in the charge on the Si(Al,O) atoms; the corresponding chemical shift thus becomes negligible. Obviously, eq 1 used in this approach actually describes the whole zeolite crystal.

An alternate explanation is that the influence of extraframework cations is just limited to the nearest framework Si, Al, and O atoms. When the Si/Al ratio approaches 1, in the case of X zeolites, almost every framework atom is the nearest neighbor of an alkali cation. According to the group shift concept,<sup>2</sup> all the binding energies of these framework atoms will shift to the lower

energy side with the electropositivity of the alkali cations. When the Si/Al ratio becomes higher, a portion of the framework atoms cannot find alkali cations as their nearest neighbors; the influence of alkali cations on these atoms is thus of negligible consequence. These atoms still retain high binding energies. As a combining result, the XPS peak enveloping both the nearest and other framework atoms will show less shift in binding energies. Finally, in high-silica zeolites, the concentration of alkali cations is so small that most of the framework atoms are free from their influence and high binding energies are still observed in this case. Apparently, according to our explanation, the framework atoms near the alkali cations will become cation characteristic. Particularly when the zeolite sample contains two kinds of alkali cations, two different shifts in binding energies should be in principle present for the same framework element. This corollary is well confirmed for N<sub>1s</sub> in the following pyrrole adsorption experiments and will be discussed below for the other elements.

The framework oxygens adjacent to alkali cations should be regarded as the Lewis basic sites. A strong collinear NH-O-bonded complex will be formed between the acidic chemisorbed pyrrole and the basic framework oxygen.<sup>13</sup> This will result in a significant bathochromic shift of the infrared NH stretching band and also in the shift of the N<sub>1s</sub> level of the pyrrole molecule

(12) Sanderson, R. T. *Chemical Bonds and Bond Energy*; Academic Press: New York, 1976.

(13) Jones, R. A.; Bean, G. P. *The Chemistry of Pyrrole*; Academic Press: London, 1977.

Table II. Deconvolution of XPS  $N_{1s}$  Peaks of Chemisorbed Pyrrole (Binding Energy, eV)

	sample					assignment
	LiX	NaX	KX	RbX	CsX-2	
component 1	399.7	399.8	399.8	399.8	399.7	species on basic sites adjacent to sodium cations
area %	37.3	87.0	44.0	46.3	51.3	
component 2	400.3	399.8	399.1	398.7	398.3	species on basic sites adjacent to other alkaline cations
area %	50.4	87.0 <sup>a</sup>	43.7	37.1	41.0	
component 3	401.5	401.5	401.5	401.6	401.5	see text
area %	12.3	13.0	12.3	16.6	7.7	

	sample					assignment
	LiY	NaY	KY	RbY	CsY	
component 1	400.5	400.5	400.7	400.5	400.6	species on basic sites adjacent to sodium cations
area %	43.8	70.9	40.2	59.8	43.5	
component 2	401.2	400.5	399.6	399.3	398.9	species on basic sites adjacent to other alkaline cations
area %	26.2	70.9 <sup>a</sup>	42.3	40.2	47.7	
component 3	399.1	399.0	<i>b</i>		<i>b</i>	polymerization product
area %	30.0	29.1				

<sup>a</sup>The same as component 1. <sup>b</sup>Weak components were found at 403.4 eV for KY and 403.5 eV for CsY, respectively. The former is due to the contribution from  $K_{2s}$  (17.5%); the source of the weak peak (8.8%) in the case of CsY remains unresolved.

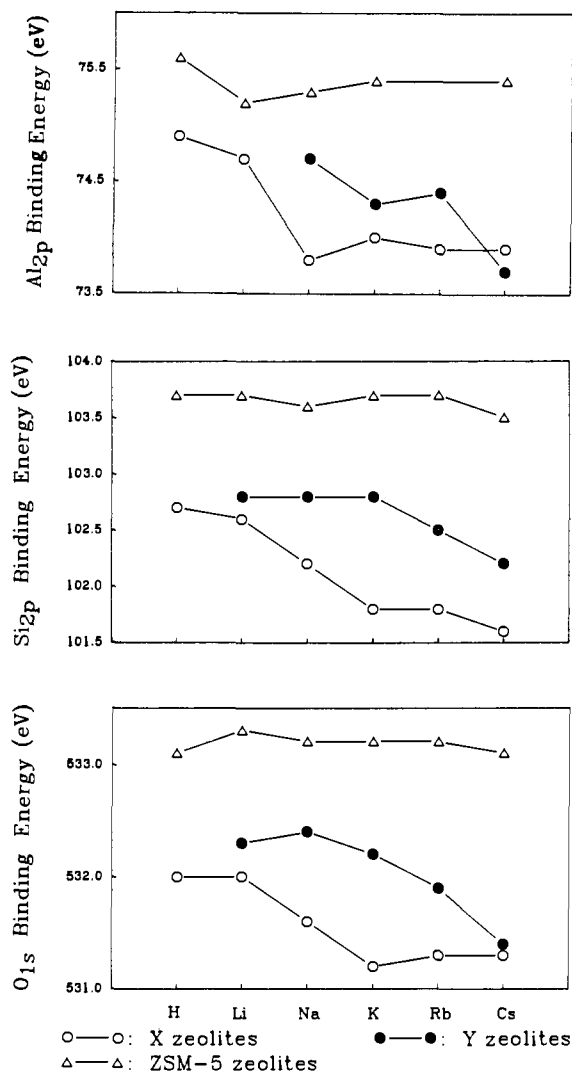


Figure 2. Chemical change in binding energies of zeolite framework elements with the extraframework cations.

in XPS spectroscopy when the basic strength of these sites increases. Our previous infrared results<sup>10</sup> indicated that the shift of NH frequency strongly depends on the counteranion in the zeolite. The coexistence of two kinds of alkali cations produces two different NH bands in the same zeolite sample. This fact suggests that the basic properties in zeolites are mainly determined by the local environment rather than the bulk zeolite lattice. The XPS study<sup>14</sup> of pyrrole chemisorbed on the alkali-cation faujasite

zeolites also showed a similar effect. Table I reveals that the  $N_{1s}$  peak is substantially broader (40–70% larger in fwhm) than the  $S_{2p}$ ,  $Al_{2p}$ , and  $O_{1s}$  levels. The  $N_{1s}$  envelopes were then deconvoluted into two or three components (Table II). It is noted that a common component with binding energy at 399.8 eV was present in the spectra of all X zeolite samples; this component peak contributed about 90% to the spectrum area of the NaX sample. Another weak but also common component was found at 401.5 eV for most of the samples. This peak usually contributed about 10% to the total  $N_{1s}$  envelope area. There is another main  $N_{1s}$  component (except for the case of the NaX sample) besides these common peaks in all the spectra, which changed significantly in binding energy with the counteranions; that is, the binding energy of this component decreased in the order  $Li > Na$  (taking the common component which contributed 90% to the spectrum area of NaX)  $> K > Rb > Cs$  and the difference in binding energy between LiX and CsX reached 2 eV. According to the assignment of infrared bands, the common component with binding energy at 399.8 eV was thus attributed to the pyrrole species chemisorbed on the same kind of basic sites associated with Na cations, while the other main component characterized the basic sites adjacent to other alkaline cations. Another weak but common component peak indicates the presence of another common adsorbed pyrrole species in all X zeolites. The relatively high binding energy (401.5 eV) suggests that it would be a weakly adsorbed pyrrole species. This band was tentatively assigned to a pyrrole species adsorbed on weaker basic sites, such as the framework oxygen not directly adjacent to a cation.

The situation of Y zeolites is similar (Table II). A common component peak can be found with binding energy around 400.6 eV in the spectra of all samples. Likewise, there is another  $N_{1s}$  component besides the common peak in the spectra (this component is the same as the common peak in the spectrum of NaY), which changed its binding energy with the counteranions in the order  $Li > Na > K > Rb > Cs$ . Similarly, here the common peak in XPS at 400.6 eV was attributed to chemisorbed pyrrole on framework oxygens adjacent to Na cations, while the other component characterized the basic sites adjacent to other alkali cations. However, differences in spectrum deconvolution were noticed in the case of NaY and LiY samples. In addition to the peaks discussed above, there is another main component peak with a lower binding energy at 399.1 eV. On the basis of the previous infrared results, this component is assigned to the slight polymerization of pyrrole which occurred only over these two samples, LiY and NaY.

The coexistence of two  $N_{1s}$  peaks in XPS spectra offers evidence that the framework oxygen adjacent to the alkali cation is the basic site, which is therefore cation characteristic. Vice versa, the influence of the cation is only limited to the adjacent framework atoms. Since a collinear NH–O-bonded complex will be formed

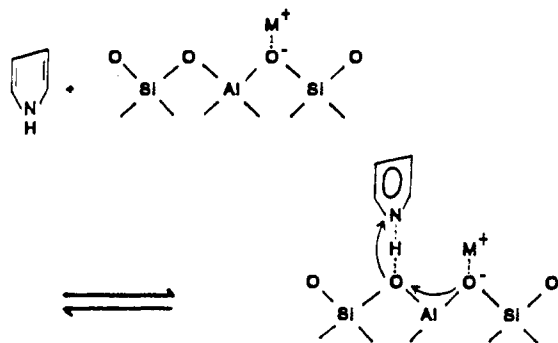


Figure 3. Model for pyrrole chemisorbed on a basic site.

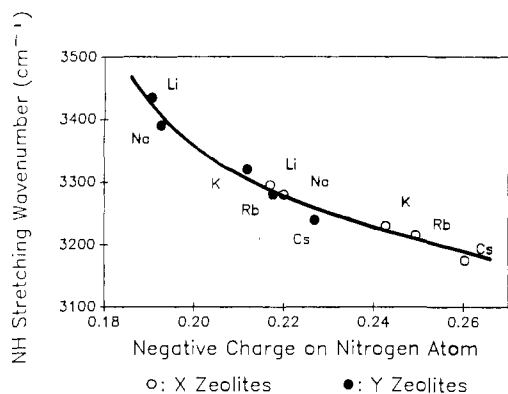


Figure 4. Relationship between the charge on the nitrogen atom and the NH stretching wavenumber of the chemisorbed pyrrole molecule.

between chemisorbed pyrrole and the basic framework oxygen, the model for pyrrole adsorption is the one drawn in Figure 3. The intermediate electronegativity can still be calculated using Sanderson's method; however, owing to the differences between local and bulk composition, we propose to introduce the following changes in the calculations. Because the cation in the supercage of faujasite is mainly located near the six oxygen rings,<sup>15</sup> in the case of a monovalent cation M, the local composition after pyrrole adsorption may be approximated as  $\text{Si}_{6-n}\text{Al}_n\text{O}_{12}\text{M}_n(\text{C}_4\text{H}_5\text{N})_n$ . The intermediate electronegativity for this hypothetical compound would be

$$S_{\text{int}} = (S_{\text{Si}}^{6-n} S_{\text{Al}}^n S_{\text{O}}^{12} S_{\text{M}}^n S_{\text{C}}^{4n} S_{\text{H}}^{5n} S_{\text{N}}^n)^{1/(18+11n)} \quad (3)$$

Then according to the electronegativity equivalent method,<sup>12</sup> the partial charge on the nitrogen can be calculated using eq 2. The calculated charge correlates well with the NH stretching frequencies observed in infrared spectra, which confirms the formation of the NH-O-bonded complex between chemisorbed pyrrole and the basic framework oxygen (Figure 4). The calculated charge also correlates well with the  $\text{N}_{1s}$  binding energies, yielding two straight lines (Figure 5a). Moreover, the two straight lines for X and Y zeolites possess the same slope, though the intercepts of these lines are slightly different. The chemical shift of the core levels in XPS is approximately described as<sup>16</sup>

$$\Delta \text{BE} = B - B_0 = k\Delta q - \Delta V \quad (4)$$

where  $B_0$  is the binding energy of the neutral atom,  $\Delta q$  denotes a change in the electron charge,  $\Delta V$  shows the Madelung potential and here mainly depends on the crystal structure and the Si/Al ratio of zeolites, and  $k$  is a constant depending on the element and proportional to  $e^2/r$  ( $r$  is the radius of the valence shell). For the same element,  $k$  should be identical and this is why the two lines in Figure 5 have the same slope.  $k$  is then equal to  $-41.6$  eV/electron for  $\text{N}_{1s}$ . Similar calculations were also done for

Binding Energy (eV)

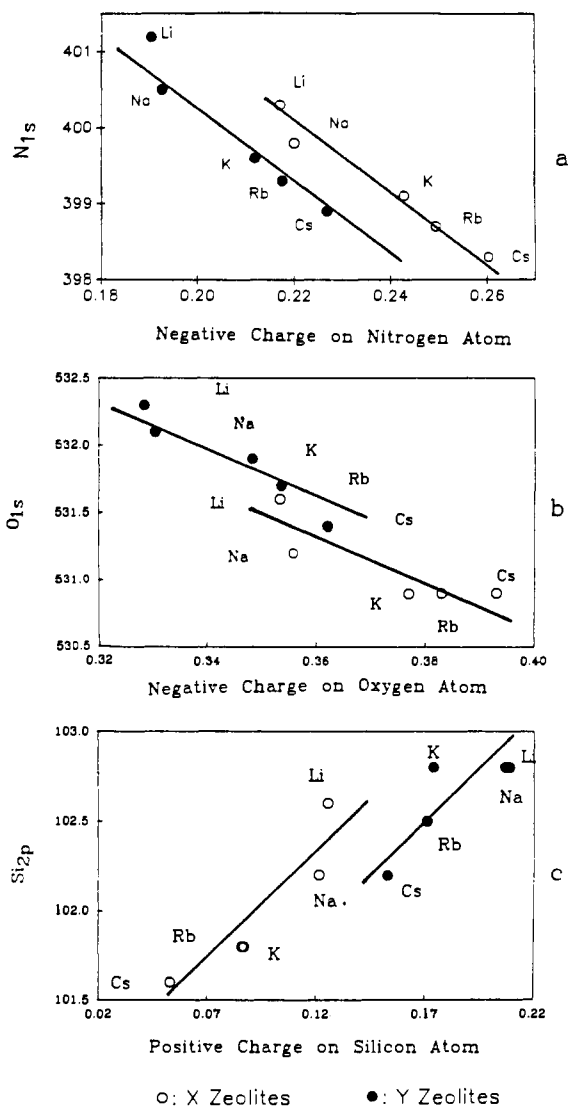


Figure 5. Relationship between charge and binding energy.

framework oxygen and silicon atoms (Figure 5b,c). The straight lines can still be drawn, and the constant  $k$  is  $-19.4$  and  $7.0$  eV/electron for  $\text{O}_{1s}$  and  $\text{Si}_{2p}$ , respectively. However, the data are widely scattered and the straight-line fitting is not as good as in the case of  $\text{N}_{1s}$ . The scattering of data is not only due to experimental errors. The charge calculated using eq 3 is responsible for the local composition around one kind (the main kind) of cation, while the binding energy adopted in Figure 5b,c is actually the envelope peak value of the XPS spectra. According to the above discussion, this envelope should also contain different kinds of binding energies which correspond to different local compositions. The narrow fwhm of  $\text{Si}_{2p}$  and  $\text{O}_{1s}$  makes the deconvolution difficult (the reason will be discussed below). Thus, the fitting in Figure 5b and c should be worse than that in Figure 5a.

Taking  $\Delta V$  as a constant for the same zeolite samples, with a fixed  $\Delta q$  the range of binding energy is mainly determined by the absolute value of constant  $k$ . Therefore, the chemical shift in the order  $\text{O}_{1s} > \text{Si}_{2s} > \text{Na}_{1s} > \text{Al}_{2p}$  observed by many authors can be explained by the relative change in absolute value of the corresponding constant  $k$ . In our case,  $k$  reduced in the order  $\text{N}_{1s} \gg \text{O}_{1s} > \text{Si}_{2p}$ . The large constant  $k$  for  $\text{N}_{1s}$  reported here strongly suggests that the probe molecules containing N atoms are useful indicators of charge transfer in XPS experiments. Our previous work using pyridine to detect acidity in zeolites<sup>11,17</sup> also confirmed

(15) Breck, D. W. *Zeolite Molecular Sieves*; Wiley-Interscience: New York, 1974.

(16) Carlson, T. A. *Photoelectron and Auger Spectroscopy*; Plenum: New York, 1975.

(17) Borade, R.; Adnot, A.; Kaliaguine, S. *J. Chem. Soc., Faraday Trans.* 1990, 86, 3949.

Table III

fitting BE	zeolite X		zeolite Y	
	<i>k</i> , eV/electron	$\Delta V$ , eV	<i>k</i> , eV/electron	$\Delta V$ , eV
N <sub>1s</sub>	-41.6	-7.4	-41.6	-6.6
O <sub>1s</sub>	-19.4	-3.4	-19.4	-3.7
Si <sub>2p</sub>	+7.0	-2.9	+7.0	-2.4

that the N<sub>1s</sub> level is sensitive to charge transfer. Vice versa, the relatively small constant *k* of O<sub>1s</sub> and Si<sub>2p</sub> will result in a small chemical shift in binding energy. Thus the fwhm of these lines is still narrow, even though each line consists of several XPS peaks with different chemical shifts.

Further information can be drawn from the intercept *I* of the line in Figure 5, that is

$$\Delta V = B_0 - I \quad (5)$$

Equation 5 offers a simple way to determine the Madelung energy of the zeolite lattice from experimental data, provided the binding energy of the corresponding neutral atom is known. The N<sub>1s</sub><sup>0</sup>, Si<sub>2p</sub><sup>0</sup>, and O<sub>1s</sub><sup>0</sup> energies are roughly approached by the values in Me<sub>4</sub>NCl (402.0 eV), Si (98.5 eV), and PhOCOPh (535.0 eV)<sup>7</sup> compounds, respectively. The calculated  $\Delta V$  values and also the measured constant *k* values are listed in Table III. The X zeolites

possess slightly larger  $\Delta V$  values than Y zeolites, which is consistent with the fact that higher Al content in zeolites produces more negative charges on the framework. Hence the contribution from Coulombic interaction between framework and extra-framework cations increases, which will result in an increase of the total Madelung energy. The Madelung energy of the potassium zeolite X was calculated theoretically using a PLUTO program.<sup>18</sup> The average Madelung energy calculated using this method is about -14.7 eV for cations located at site II. This value is higher than our results but still comparable. The high value obtained by the PLUTO method might be due to the ionic crystal model for the zeolite lattice employed in the calculation, since the real zeolite lattice is only partially ionic.<sup>1</sup>

In summary, the XPS study suggests that the framework-cation interaction in alkali-cation-exchanged zeolites is limited to a short-range scope. The probe molecules containing N atoms are sensitive indicators of charge transfer in XPS experiments. The Si<sub>2p</sub> binding energy level is not a good internal reference binding energy in XPS spectra for zeolites possessing low Si/Al ratios.

Registry No. Pyrrole, 109-97-7.

(18) Sanders, M. J.; Catlow, C. R. A. *Proceedings of 6th International Zeolite Conference*, Olson, D., Bisio, A., Eds.; Butterworths: Guildford, U.K., 1983; p 131.

## Ab Initio Molecular Orbital Conformational Analysis of Prototypical Organic Systems. 1. Ethylene Glycol and 1,2-Dimethoxyethane

Mark A. Murcko\*<sup>†</sup> and Raymond A. DiPaola<sup>‡</sup>

Contribution from Vertex Pharmaceuticals Incorporated, 40 Allston Street, Cambridge, Massachusetts 02139-4211, and Computer Center, Fairfield University, Fairfield, Connecticut 06430. Received October 29, 1990

**Abstract:** Ab initio calculations have been used to study the changes in energy of ethylene glycol and 1,2-dimethoxyethane as a function of rotation around the central C-C bond. Geometries have been fully optimized at the 3-21G and 6-31G\* levels, and single-point calculations have been carried out at higher levels (up to 6-311++G\*\* for ethylene glycol and 6-31+G\* for 1,2-dimethoxyethane), including electron correlation up to MP4(SDTQ). For ethylene glycol, the H-O-C-C angles were started in a trans orientation to prevent intramolecular hydrogen bonding. In 1,2-dimethoxyethane, the C-O-C-C dihedral angles also were started in the trans orientation. At all levels of theory, both ethylene glycol and 1,2-dimethoxyethane slightly prefer a trans O-C-C-O orientation. For both molecules, the 3-21G relative energies are quite different from those calculated at the 6-31G\* level, but all larger basis sets give relative energies which agree fairly well with the 6-31G\* results. Electron correlation is shown to have a significant effect on the relative energies. The highest-level calculations for both ethylene glycol and 1,2-dimethoxyethane indicate that the trans-gauche energy difference is 0.4-0.5 kcal/mol. However, these values decrease as the basis set is increased, and, in the limits of infinite basis set and complete treatment of electron correlation, the trans-gauche difference for both molecules should be somewhat lower. Vibrational frequencies have been calculated for all conformers of both ethylene glycol and 1,2-dimethoxyethane; the effect of zero-point energies and vibrational enthalpies on the trans-gauche energy difference are quite small, but there is a more significant lowering of the barrier heights. To judge the importance of intramolecular hydrogen bonding in ethylene glycol, several lower-energy gauche O-C-C-O conformers which do possess intramolecular hydrogen bonds also were located. The global minimum has one H-O-C-C angle gauche and the other H-O-C-C angle trans, in agreement with experiment. The trans-trans-gauche conformer of 1,2-dimethoxyethane, with one gauche C-O-C-C angle, also was studied and was found to be ~1.5 kcal/mol above the all-trans global minimum. For both ethylene glycol and 1,2-dimethoxyethane, the MM2 force field does a reasonable job of reproducing the trans-gauche energy differences but is in poor agreement with the ab initio syn barriers to rotation. However, the MM3 barrier heights are in much better agreement with the ab initio data. Further, most of the other conformational energy differences also are better reproduced by MM3, which in many ways appears to provide a superior treatment for these 1,2-dioxy-substituted ethane derivatives.

### Introduction

Many fundamental questions in conformational analysis may be addressed by the study of 1,2-disubstituted ethanes of the form X-C-C-Y.<sup>1</sup> These molecules may be viewed as structural

prototypes—the simplest structures which incorporate functional groups commonly found in larger systems. While it is usually the case that a trans orientation of the X-C-C-Y fragment is energetically preferred, there are cases in which there is no sig-

\* To whom correspondence should be addressed.

<sup>†</sup> Vertex Pharmaceuticals.

<sup>‡</sup> Fairfield University.

(1) Eliel, E. L.; Allinger, N. L.; Angyal, S. G.; Morrison, G. A. *Conformational Analysis*; Wiley-Interscience: New York, 1966.